Temperature-dependent properties of the magnetic order in single-crystal $BiFeO_3$

M. Ramazanoglu,[1] W. Ratcliff II,[2] Y. J. Choi,[1] Seongsu Lee,[3] S.-W. Cheong,[1] and V. Kiryukhin[1]

[1]*Department of Physics and Astronomy, Rutgers University, Piscataway, New Jersey 08854, USA*

[2]*NIST Center for Neutron Research, National Institute of Standards and Technology, Gaithersburg, Maryland 20899, USA*

[3]*Neutron Science Division, Korea Atomic Research Institute, Daejon 305-353, Korea*

(Received 17 February 2011; revised manuscript received 14 April 2011; published 23 May 2011)

We report neutron diffraction and magnetization studies of the magnetic order in multiferroic $BiFeO_3$. In ferroelectric monodomain single crystals, there are three magnetic cycloidal domains with propagation vectors equivalent by crystallographic symmetry. The cycloid period slowly grows with increasing temperature. The magnetic domain populations do not change with temperature except in the close vicinity of the Néel temperature, at which, in addition, a small jump in magnetization is observed. No evidence for the spin-reorientation transitions proposed in previous Raman and dielectric studies is found. The magnetic cycloid is slightly anharmonic for $T = 5$ K. The anharmonicity is much smaller than previously reported in nuclear magnetic resonance studies. At room temperature, a circular cycloid is observed, within errors. We argue that the observed anharmonicity provides important clues for understanding electromagnons in $BiFeO_3$.

DOI: 10.1103/PhysRevB.83.174434 PACS number(s): 75.40.Cx, 75.85.+t, 75.25.−j

I. INTRODUCTION

The coupling between ferroelectric (FE) polarization and magnetic order in solid-state materials, known as multiferroics, attracts significant interest because of its importance for understanding the properties of these materials, as well as of engineering application possibilities.[1–4] Among the known multiferroics, $BiFeO_3$ (BFO) is the only one exhibiting both magnetic and FE orders at room temperature. These orders are coupled, and control of both FE and magnetic properties by an electric field has been demonstrated in thin film and single crystal samples,[5,6] as well as discussed theoretically.[7,8] Importantly, the magnitude of the spontaneous electric polarization ($P \sim 10^2$ μC/cm^2) in BFO is very large, facilitating control by the electric field and opening possibilities for applications in multistate memory devices, spintronics, and configurable electronics.[9] Therefore, BFO attracts considerable attention compared to other multiferroics. Until recently, BFO research was limited to thin films showing rather different properties from those of the bulk samples, and to polycrystals.[1] Since suitable single crystals have become available recently, their properties were subject of many studies.[6,9–14] Some of the basic properties of BFO, however, still remain to be characterized.

The temperature-dependent evolution of the magnetic structure in BFO is an important subject with several currently unresolved issues. Below the FE transition at $T_c \sim 1150$ K, BFO exhibits an $R3c$ rhombohedral perovskite structure, which is described in this paper using a pseudo-cubic notation with $a \sim 3.96$ Å, and $\alpha \sim 89.4°$. Fe^{3+} spins order at $T_N \sim 640$ K. It has long been known that the magnetic order is of the antiferromagnetic G type, with a long-range cycloidal modulation superimposed.[15] This modulation can propagate along three directions equivalent by symmetry, described by propagation vectors $\tau_1 = \delta(1,-1,0)$, $\tau_2 = \delta(1,0,-1)$, and $\tau_3 = \delta(0,-1,1)$, where $\delta \sim 0.0045$ reciprocal lattice units (r.l.u.). For each of the three cycloids, the spins rotate in the plane defined by the (111) and τ vectors, see Figs. 1(a) and 1(b). A possibility for a so far undetected canting of the spins out of the cycloid plane has been discussed theoretically.[7] Below the room temperature, several anomalies have been observed in Raman[12,16] and dielectric susceptibility measurements.[17] Some of these anomalies, such as those at $T = 140$ K and 200 K, are quite significant. It was proposed that these anomalies were associated with putative spin reorientation transitions, which are rather common in magnetic orthoferrites.[1] We note that spin reorientation can occur through magnetic transitions within the existing magnetic domains, or through changes in the fractional populations of the equivalent magnetic domains τ_i. Nuclear magnetic resonance (NMR) measurements indicate that the spin cycloid is anharmonic at $T = 5$ K, while the anharmonicity is absent at $T = 300$ K.[18–20] However, this effect is subtle, and therefore unlikely to produce the strong anomalies at $T = 140$ K and 200 K. In any case, the NMR measurements of the magnetic order are indirect, and require confirmation. In fact, neutron diffraction studies of polycrystals did not find any measurable differences between the magnetic structures at $T = 4$ K and at the room temperature.[21] In particular, no dependence of δ on temperature was reported. So far, measurements of the magnetic order parameter and search for possible changes of the magnetic structure by direct techniques in the full temperature range, from helium temperatures up to T_N, were absent, in part due to absence of suitable single crystals. Such measurements are clearly necessary to address the questions discussed above. They are also needed to understand the character of the magnetic transition at T_N and its possible interrelationship with the FE properties of BFO. The neutron diffraction and magnetization measurements described in the current study were motivated by these needs.

II. EXPERIMENTAL DETAILS

Single crystals of $BiFeO_3$ were grown using flux method as described in Refs. 9 and 10. The crystal growth occurs below the FE transition temperature and tends to produce FE monodomain crystals. Neutron diffraction experiments were carried out on BT-9 triple-axis spectrometer at NIST Center for Neutron Research. A closed cycle cryostat and a furnace were used for temperature-dependent measurements. The neutron

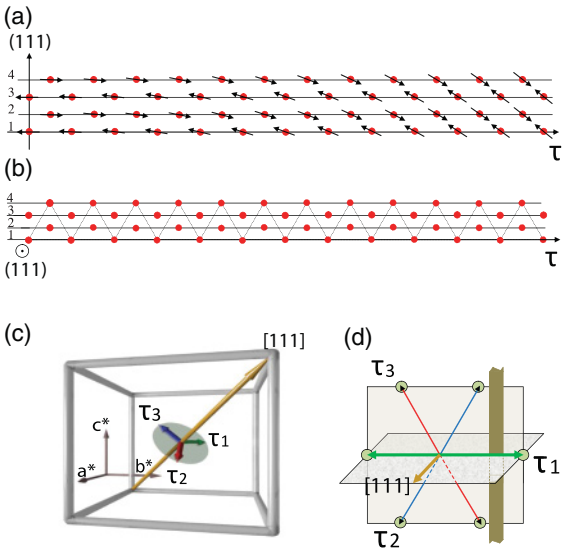

FIG. 1. (Color online) (a) Cycloidal magnetic structure of $BiFeO_3$ projected on the plane of the (111) and τ vectors. About one-tenth of the cycloid period along τ is shown. (b) View of the same Fe chains, labeled 1 through 4, projected on the plane normal to (111). (c) Pseudocubic unit cell of BFO and the magnetic modulation wave vectors τ_i originating at $Q_0 = (0.5, 0.5, 0.5)$. (d) Scattering geometry. The horizontal scattering plane contains τ_1 and (111). Circles indicate the magnetic peak positions. The experimental resolution function is sketched with a dark vertical slab.

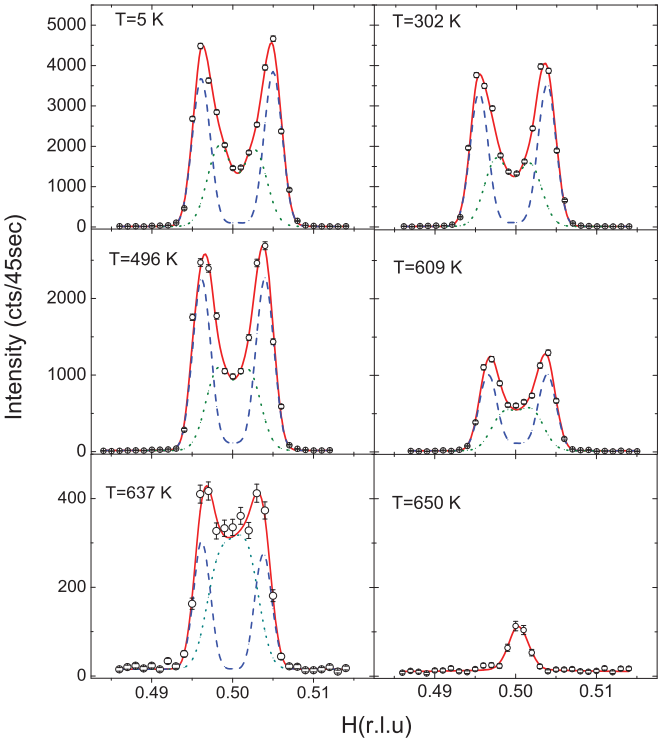

FIG. 2. (Color online) Magnetic diffraction peaks in the vicinity of $Q_0 = (0.5, 0.5, 0.5)$. The scans are centered at Q_0, and the scan direction is along (H,−H,0.5). Solid lines are results of fits discussed in the text. Dashed and dotted lines depict the calculated contributions due to the in-plane and out-of-plane magnetic domains, respectively.

energy was 14.7 meV, and collimations of 40-40-S-40-open (order parameter measurements) or 10-10-S-10-open (third harmonic studies) were used. To reduce the $\lambda/2$ contamination of the neutron beam, pyrolytic graphite filters were used before and after the sample, as well as in-pile. A $3 \times 2 \times 0.5$ mm^3 FE monodomain sample was oriented in the $[h, k, (h + k)/2]$ scattering plane. In this paper, we use the pseudocubic notation for all the reciprocal lattice vectors, which are measured in r.l.u.. Magnetization measurements were performed using a SQUID magnetometer under an applied magnetic field of 0.2 T. In all figures, error bars are from counting statistics.

III. RESULTS AND DISCUSSION

To characterize the temperature-dependent behavior of the magnetic order parameter, the periodicity of the spin cycloid, equivalent magnetic domain populations, and possible anharmonicity of the cycloid, single-crystal neutron diffraction experiments were carried out. The most intense magnetic reflection is observed at the $Q_0 \pm \tau_i$ positions, where $Q_0 =$ (0.5, 0.5, 0.5) and $i = 1,2,3$, giving rise to six diffraction peaks. The experimental scattering geometry is illustrated in Figs. 1(c) and 1(d). The horizontal scattering plane contains perpendicular vectors Q_0 and τ_1. Therefore, magnetic domain τ_1 (the in-plane domain) produces peaks at $Q_0 \pm \delta$ in the scan along the τ_1 centered at Q_0. The magnetic domains τ_2 and τ_3 (the out-of-plane domains) produce peaks in the plane normal to the scattering plane. Nevertheless, they are also captured by this scan because of the broad instrumental resolution normal to the scattering plane. As illustrated in Fig. 1(d), the out-of-plane domains produce overlapping peaks at $Q_0 \pm \delta/2$. Thus, a single scan along τ_1 at the (0.5, 0.5, 0.5) position allows us to characterize the in-plane domain, as well as to measure the combined signal of the out-of-plane domains.

The scans were taken in the temperature range from $T = 5$ K to 650 K. The scattering profiles are shown in Fig. 2 for several representative temperatures. For $T > T_N \sim 640$ K, a weak temperature-independent peak is observed at Q_0. It can originate from a $\lambda/2$ leakage in the neutron beam or reflect a previously undetected small lattice distortion at this wave vector. In the magnetic phase, two asymmetric peaks centered roughly at $Q_0 \pm \delta$ are observed. These peaks have clear shoulders in the direction of Q_0, as best seen for the $T = 5$ K data in Fig. 2. The overall peak shape is described perfectly by combined signals from the in- and out-of-plane magnetic domains at $Q_0 \pm \delta$ and $Q_0 \pm \delta/2$, respectively. This picture was confirmed by the room-temperature scans in the planes containing Q_0 and either τ_2 or τ_3 (not shown). Therefore, the scattering profiles were fitted using five Gaussian peaks: at $Q_0 \pm \delta$ (the in-plane magnetic domain), $Q_0 \pm \delta/2$ (combined out-of-plane domains), and a weak temperature-independent background peak at Q_0. The common Gaussian peak width was determined as a global parameter fitted to a common value over the entire temperature range. The intensities of the magnetic peaks, as well as the wave vector of the cycloid δ, were fitted at each temperature. This procedure resulted in high-quality fits, as shown in Fig. 2.

Figure 3(a) shows the temperature dependence of the integrated magnetic intensity, which is proportional to the square of the magnetic order parameter. It exhibits a canonical

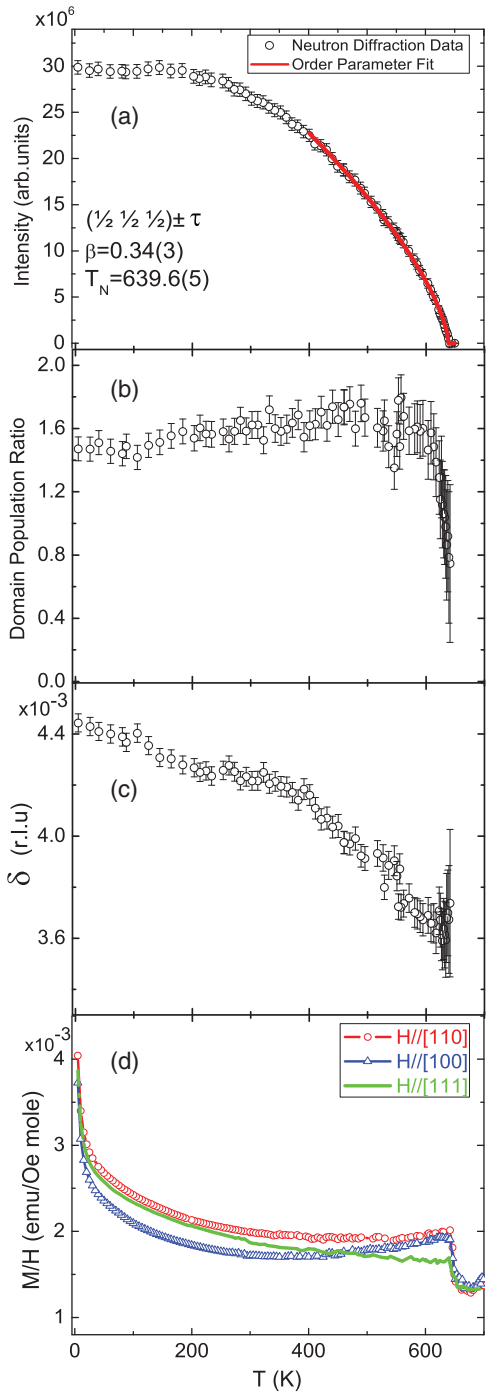

FIG. 3. (Color online) Temperature dependences of (a) the magnetic order parameter given by the integrated scattering intensity near Q_0. (b) The ratio of the population of the in-plane magnetic domain to the combined populations of the out-of-plane domains. (c) The magnitude δ of the wave vector $\delta(1,-1,0)$ of the magnetic modulation, and (d) the magnetization in the field of $H = 0.2$ T for various directions of H (1 emu/Oe $= 4\pi \times 10^{-6}$ m^3). The solid line in (a) is the result of the power-law fit discussed in the text.

second-order-like behavior and is well described by the power law $(1 - T/T_N)^{2\beta}$ in a rather large region below T_N; see Fig. 3(a). The power law gives $T_N = 639.6(5)$ K, and $\beta = 0.34(3)$. The critical exponent β is in agreement with three-dimensional magnetic transitions. A similar β value was previously found in Mössbauer studies.[22] The transition temperature T_N is within the range of previously reported values for polycrystalline samples (590–650 K)[1,23] and is consistent with theoretical predictions.[24] The ratio of the integrated intensity of the magnetic peaks at $Q_0 \pm \delta$ to that at $Q_0 \pm \delta/2$ gives the ratio of the in-plane and the out-of-plane domain populations. This ratio is shown in Fig. 3(b) as a function of temperature. Except for the narrow vicinity of the magnetic transition temperature, this ratio is essentially constant. As T_N is approached, the ratio decreases from about 1.5 to 0.8, i.e., the relative population of the out-of-plane domains grows. This observation may reflect increased significance of thermal fluctuations for $T \sim T_N$. The magnitude of the cycloidal modulation wave vector δ decreases with temperature, as shown in Fig. 3(c). The corresponding modulation period grows from 629(5) Å at $T = 5$ K to 780(30) Å at $T = 615$ K. There is an apparent change of slope of this temperature dependence at $T \sim 400$ K. In previous works,[21] the measurements were done in a smaller temperature range, and no temperature dependence of δ was reported.

Figure 3(d) shows the temperature dependence of the magnetization, with the magnetic field applied along different crystallographic directions. The general behavior below T_N is consistent with an antiferromagnet containing a small ferromagnetic impurity fraction. Similar behavior was reported elsewhere.[1,25] The anomaly at T_N itself is, however, rather unusual. The abrupt upward magnetization jump that accompanies appearance of the magnetic order is seemingly inconsistent both with the otherwise second-order-like behavior of the magnetic order parameter, and with the antiferromagnetic transition. The magnetization jump is rather small, corresponding to effective magnetic moment of $\sim 5 \times 10^{-4}$ μ_B/spin in the applied field of 0.2 T. This suggests that the spin component involved in the abrupt transition is small, which is consistent with the order parameter behavior of Fig. 3(a). Interestingly, the distribution of the magnetic domain populations also exhibits an abrupt change in the same temperature region. These data suggest that the magnetic structure of BFO is more complex than currently believed or that nontrivial effects related to the magnetic domains occur near the magnetic transition temperature. The symmetry of the magnetic structure is a key factor defining possible magnetoelectric effects, such as existence of linear magnetoelectric coupling.[26] Further study of the nature of the transition at T_N is, therefore, of significant interest.

Deviations of the magnetic structure from the circular cycloid have been detected previously but only at cryogenic temperatures. Specifically, line shapes observed in NMR spin-echo measurements at $T = 5$ K are inconsistent with this structure.[18–20] The NMR results were explained using an anharmonic cycloidal spin structure, which results from magnetic anisotropy in the plane of the spin rotation. The free-energy density in BFO can be written[26] in the form $f = f_L + f_{\text{exch}} + f_{\text{an}}$. Here f_L is the relativistic inhomogeneous magnetoelectric interaction, $f_{\text{exch}} = A \sum (\nabla l_i)^2$ $(i = x,y,z)$ is the inhomogeneous exchange energy with exchange stiffness A, $f_{\text{an}} = K_u \sin^2(\theta)$ is the anisotropy energy with the anisotropy constant K_u, $\mathbf{l}$ is the antiferromagnetic vector, and θ is the angle between $\mathbf{l}$ and the (111) direction. The solution of this model is an anharmonic cycloid in which

the spin component along the (111) direction is given by the elliptic Jacobi function $sn(4K(m)x/\lambda,m)$, where m is its parameter, $K(m)$ is the complete elliptic integral of the first kind, λ is the modulation period, and x designates the propagation direction.[26] Depending on the parameter m, the spin modulation changes from purely circular ($m = 0$) to a square wave in which the spins bunch along the (111) direction ($m = 1$). NMR line-shape analysis based on this model indicated that the spin cycloid is strongly distorted at $T = 5$ K ($m = 0.95$), whereas it becomes essentially circular at room temperature ($m = 0.48$).[18–20]

The magnetic neutron diffraction signal is produced by the spin components normal to the scattering vector. In our experiment, the scattering vector is essentially parallel to (111), and therefore only the spin components along the cycloid propagation vector τ contribute to scattering. These components are given by $[1 - sn^2(4K(m)x/\lambda,m)]^{0.5} = cn(4K(m)x/\lambda,m)$. The diffraction intensity is proportional to the square of the Fourier transform of the magnetization density. The Jacobi function has only odd harmonics in its Fourier series, and therefore scattering from the anharmonic cycloid described above should produce peaks at $Q_0 \pm n\tau$ (n is odd), whose intensity is proportional to the square of the appropriate Fourier coefficient. The ratio of these coefficients depends only on m. Thus, the ratio of the integrated intensities of the first ($n = 1$) to the third ($n = 3$) harmonics of the magnetic peak, I_1/I_3, provides direct measurement of m. Figure 4(a) shows high-resolution scans capturing the $Q_0 - \tau_1$ and $Q_0 - 3\tau_1$ positions, taken at $T = 5$ K and 300 K. A barely discernible third harmonic appears to be present at $T = 5$ K, while none is seen at $T = 300$ K. The data in Fig. 4(a) were fitted using the model described above with the third harmonic peak added, and the line shapes changed to the resolution-corrected pseudo-Voigt function to correctly describe the wings of the peaks. For $T = 5$ K, the fit gives $I_1/I_3 = 500 \pm 100$, corresponding to $m = 0.50$, and for $T = 300$ K $I_1/I_3 > 2000$. The obtained $m = 0.50$ produces only a very small deviation from the circular cycloid structure, as illustrated in Fig. 4(b) and in the inset in Fig. 4(a). In contrast, the value of $m = 0.95$ derived from the NMR data at $T = 5$ K would imply a clear bunching of spins along the (111) direction, see Fig. 4(c). We note, however, that $m = 0.95$ would give $I_1/I_3 \sim 25$, which is clearly inconsistent with our results. Neutron diffraction provides a more direct method for measuring the anharmonicity than NMR, and therefore we conclude that the low-temperature cycloid is more harmonic than previously reported. Both of these techniques indicate that the cycloid is essentially circular at room temperature.

The anisotropy energy K_u is related[19] to m by $K_u = 16mAK^2(m)/\lambda^2$. The literature values of the exchange stiffness A are in the range of $(2–4) \times 10^{-14}$ J/cm. [18,19,27–30] Using $m = 0.50$, one obtains $K_u = (1.5–3) \times 10^{-2}$ J/cm^3 $= (0.6 - 1.2) \times 10^{-5}$ eV/spin. This is about 4 times smaller than that obtained using the NMR value of m and 2 times smaller than the value found using ESR.[31] We note that the magnetic anisotropy is comparable to the inhomogeneous exchange energy $E_{\text{exch}} \sim A\delta^2$ since $K_u/(A\delta^2) = 4mK^2(m)/\pi^2 = 0.7$ for $m = 0.50$. Both of these energies are smaller than kT, and therefore the anharmonic cycloid can be significantly affected by thermal fluctuations. This could explain, in particular, the apparent disappearance of the third harmonic peak at high temperatures, since the fluctuation-induced peak broadening often increases with the harmonic order,[32,33] and any broadening of the already small peak would render it immeasurable.

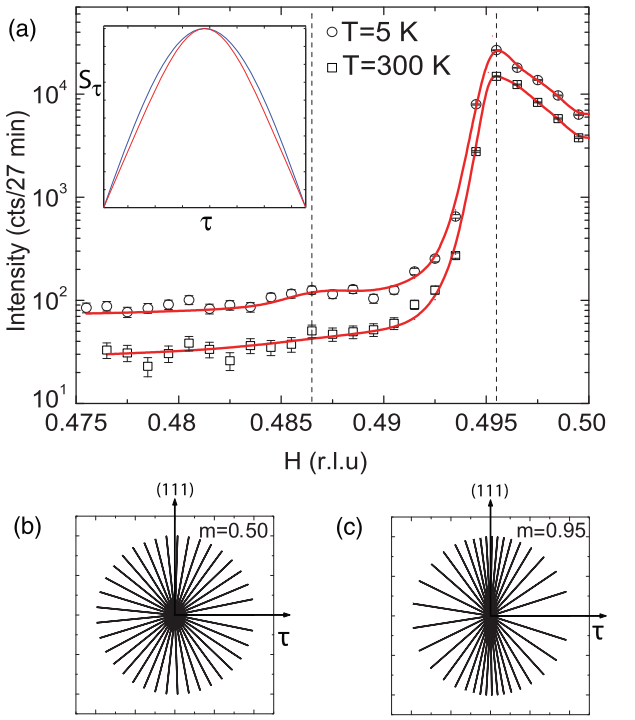

FIG. 4. (Color online) (a) Magnetic diffraction peak profiles for $T = 5$ K and 300 K on a logarithmic scale. Solid lines depict results of fits discussed in the text. Dashed lines indicate positions of the first and third harmonics. The $T = 300$ K scan is shifted down for clarity. The inset shows the spatial variation of the spin component S_τ along the modulation propagation direction τ for the circular cycloid with $m = 0$ (top curve) and for the anharmonic cycloid at $T = 5$ K with $m = 0.50$ (bottom curve). (b) Fe spins in the anharmonic cycloid with experimentally determined $m = 0.50$ plotted from the same origin. For clarity, only one-third of all spins are shown. (c) The same as (b) but for $m = 0.95$. Our results are inconsistent with the latter value.

Anharmonicity of the spin cycloid is an important parameter defining dynamical magnetoelectric response. It determines which spin wave branches couple to the electric polarization, giving rise to hybrid excitations (electromagnons). It was predicted, for instance, that the cyclone magnon mode ϕ_2 and the extracyclone magnon mode ψ_3 only have the hybrid character in the presence of the third harmonic in the cycloid.[34] Higher-order harmonics make other cycloidal spin modes hybrid. Such spin modes have been observed in BFO.[12] Importantly, they have been found to exhibit giant energy shifts in an applied electric field, indicating a significant magnetoelectric coupling.[14] Our measurements of the cycloid anharmonicity and of the relevant magnetic interaction energies should provide valuable input for microscopic description of the excitation modes and of the observed giant magnetoelectric effects in BFO.

As discussed above, various anomalies have been observed below room temperature in Raman and dielectric property

studies. Some of these anomalies were attributed to putative magnetic transitions. We do not observe any changes in the magnetic structure for $T < 300$ K, except for a slow and gradual change of the cycloid periodicity. Other recent neutron data are in agreement with these results.[35] Our data therefore show that the reported anomalies are not related to any magnetic transition, with only possible exception being a sudden change in the magnetic domain populations at these temperatures. While the temperature-dependent behavior of the domain populations could certainly be sample dependent, the observed absence of such a change in our samples makes the latter scenario appear unlikely. Other physical mechanisms should therefore be sought to explain the reported anomalies.

IV. CONCLUSIONS

To summarize, we report neutron diffraction and magnetization studies of the magnetic properties of single-crystal $BiFeO_3$ in the temperature range from $T = 5$ K to the temperatures exceeding T_N. The magnetic order parameter exhibits a smooth second-order-like dependence typical of the three-dimensional magnetic transition. On the other hand, the magnetization exhibits a small jump at T_N, which is seemingly inconsistent with a regular antiferromagnetic transition. The reason for this behavior is yet to be determined. The period of the magnetic modulation smoothly increases with temperature from 630 Å at $T = 5$ K to ~780 Å near T_N, exhibiting a change of slope at $T \sim 400$ K. The populations of the magnetic domains do not change with temperature, except in the close vicinity of T_N. There is a very small anharmonicity in the magnetic cycloid at $T = 5$ K (the Jacobi function parameter $m = 0.50$), which becomes undetectable at room temperature. It is significantly smaller than that reported in previous NMR studies.[18–20] The magnetic anisotropy energy derived from the observed anharmonicity is $K_u \sim 10^{-5}$ eV/spin, it is comparable to the inhomogeneous exchange energy. The observed anharmonic parameters bear relevance for understanding the nature of hybrid excitations,[34] as well as provide input for understanding the giant effects[14] of an electric field on the spin dynamics of $BiFeO_3$. No magnetic anomalies have been found below the room temperature. We therefore conclude that the anomalies previously observed in Raman[1,12,16] and dielectric measurements[17] are not related to spin-reorientation transitions.

ACKNOWLEDGMENTS

This work was supported by the NSF under Grant Nos. DMR-1004568 and DMR-0804109.

[1] For a review, see G. Catalan and J. F. Scott, Adv. Mater. **21**, 2463 (2009).
[2] S -W. Cheong and M. Mostovoy, Nat. Mater. **6**, 13 (2007).
[3] A. K. Zvezdin and A. A. Mukhin, JETP Lett. **89**, 328 (2009).
[4] R. Ramesh and N. A. Spaldin, Nat. Mater. **6**, 13 (2007).
[5] T. Zhao *et al.*, Nat. Mater. **5**, 823 (2006).
[6] S. Lee, W. Ratcliff II, S.-W. Cheong, and V. Kiryukhin, Appl. Phys. Lett. **92**, 192906 (2008).
[7] C. Ederer and N. A. Spaldin, Phys. Rev. B **71**, 060401 (2005).
[8] S. Lisenkov, D. Rahmedov, and L. Bellaiche, Phys. Rev. Lett. **103**, 047204 (2009).
[9] T. Choi, S. Lee, Y. J. Choi, V. Kiryukhin, and S.-W. Cheong, Science **324**, 63 (2009).
[10] S. Lee, T. Choi, W. Ratcliff II, R. Erwin, S.-W. Cheong, and V. Kiryukhin, Phys. Rev. B **78**, 100101(R) (2008).
[11] D. Lebeugle, D. Colson, A. Forget, M. Viret, A. M. Bataille, and A. Goukasov, Phys. Rev. Lett. **100**, 227602 (2008).
[12] M. Cazayous, Y. Gallais, A. Sacuto, R. de Sousa, D. Lebeugle, and D. Colson, Phys. Rev. Lett. **101**, 037601 (2008).
[13] P. Rovillain, M. Cazayous, Y. Gallais, A. Sacuto, R. P. S. M. Lobo, D. Lebeugle, and D. Colson, Phys. Rev. B **79**, 180411(R) (2009).
[14] P. Rovillain, R. de Sousa, Y. Gallais, A. Sacuto, M. A. Measson, D. Colson, A. Forget, M. Bibes, A. Barthelemy, and M. Cazayous, Nat. Mater. **9**, 975 (2010).
[15] I. Sosnowska, T. Peterlin-Neumaier, and E. Steichele, J. Phys. C: Solid State Phys. **15**, 4835 (1982).
[16] M. K. Singh, R. S. Katiyar, and J. F. Scott, J. Phys. Condens. Matter **20**, 252203 (2008).
[17] S. A. T. Redfern, C. Wang, J. W. Hong, G. Catalan, and J. F. Scott, J. Phys. Condens. Matter **20**, 452205 (2008).
[18] A. V. Zalesskii, A. A. Frolov, A. K. Zvezdin, A. A. Gippius, E. N. Morozova, D. F. Khozeev, A. S. Bush, and V. S. Pokatilov, JETP **95**, 101 (2002).
[19] A. V. Zalesskii, A. K. Zvezdin, A. A. Frolov, and A. S. Bush, JETP Lett. **71**, 465 (2000).
[20] A. A. Bush, A. A. Gippius, A. V. Zalesskii, and E. N. Morozova, JETP Lett. **78**, 389 (2003).
[21] R. Przenioslo, A. Palewicz, M. Regulski, I. Sosnowska, R. M. Ibberson, and K. S. Night, J. Phys. Condens. Matter **18**, 2069 (2006).
[22] C. Blaauw and F. van der Woude, J. Phys. C **6**, 1422 (1973).
[23] P. Fisher, M. Polomska, I. Sosnowska, and M. Szymansky, J. Phys. C **13**, 1931 (1980).
[24] D. Albrecht, S. Lisenkov, Wei Ren, D. Rahmedov, Igor A. Kornev, and L. Bellaiche, Phys. Rev. B **81**, 140401(R) (2010).
[25] M. K. Singh, W. Prellier, M. P. Singh, R. S. Katiyar, and J. F. Scott, Phys. Rev. B **77**, 144403 (2008).
[26] A. M. Kadomtseva, A. K. Zvezdin, Yu. F. Popov, A. P. Pyatakov, and G. P. Vorobev, JETP Lett. **79**, 571 (2004).
[27] A. V. Zalessky, A. A. Frolov, T. A. Khimich, A. A. Bush, V. S. Pokatilov, and A. K. Zvezdin, Europhys. Lett. **50**, 547 (2000).
[28] A. G. Zhdanov, T. B. Kosykh, A. P. Pyatakov, A. K. Zvezdin, and D. Viehland, J. Magn. Magn. Mater. **300**, e437 (2006).
[29] A. S. Logginov, G. A. Meshkov, A. V. Nikolaev, A. P. Pyatakov, V. A. Shust, A. G. Zhdanov, and A. K. Zvezdin, J. Magn. Magn. Mater. **310**, 2569 (2007).
[30] I. Sosnowska and A. K. Zvezdin, J. Magn. Magn. Mater. **140-144**, 167 (1995).
[31] B. Ruette, S. Zvyagin, A. P. Pyatakov, A. Bush, J. F. Li, V. I. Belotelov, A. K. Zvezdin, and D. Viehland, Phys. Rev. B **69**, 064114 (2004).

[32] A. Aharony, R. J. Birgeneau, C. W. Garland, Y.-J. Kim, V. Lebedev, R. Netz, and M. Young, Phys. Rev. Lett. **74**, 5064 (1995).

[33] R. J. Christianson, Y. J. Wang, S. C. LaMarra, R. J. Birgeneau, V. Kiryukhin, T. Masuda, I. Tsukada, K. Uchinokura, and B. Keimer, Phys. Rev. B **66**, 174105 (2002).

[34] R. de Sousa and J. E. Moore, Phys. Rev. B **77**, 012406 (2008).

[35] J. Herrero-Albillos, G. Catalan, J. A. Rodriguez-Velamazan, M. Viret, D. Colson, and J. F. Scott, J. Phys. Condens. Matter **22**, 256001 (2010).